Journal of the Association of Arab Universities for Basic and Applied Sciences (2016) **21**, 10–16

University of Bahrain

Journal of the Association of Arab Universities for Basic and Applied Sciences

www.elsevier.com/locate/jaaubas
www.sciencedirect.com

ORIGINAL ARTICLE

Synthesis, characterization and in vitro drug release of cisplatin loaded Cassava starch acetate–PEG/gelatin nanocomposites

V. Raj *, G. Prabha

Advanced Materials Research Laboratory, Department of Chemistry, Periyar University, Salem 11, Tamil Nadu, India

Received 27 April 2015; revised 6 August 2015; accepted 23 August 2015
Available online 19 November 2015

KEYWORDS

Cassava starch acetate;
Drug delivery;
Polyethylene glycol (PEG);
Gelatin;
Cisplatin;
Nanocomposites

Abstract The aim of the present study is to examine the feasibility of Cassava starch acetate (CSA)–polyethylene glycol (PEG)–gelatin (G) nanocomposites as controlled drug delivery systems. It is one of the novel drug vehicles which can be used for the controlled release of an anticancer drug. Simple nano precipitation method was used to prepare the carriers CSA–PEG–G nanocomposites and they were used for entrapping cisplatin (CDDP). Through FT-IR spectroscopy, the linking among various components of the system was proved and with the help of scanning electron microscope and transmission electron microscopy (TEM), the surface morphology was investigated. The particle sizes of the CSA–CDDP, CSA–CDDP–PEG and CSA–CDDP–PEG–G polymer composites were between 140 and 350 nm, as determined by a Zetasizer. Drug encapsulation efficiency, drug loading capacity and in vitro release of CDDP were evaluated respectively. The findings revealed that the cross linked CSA–PEG–G nanocomposites can be a potential polymeric carrier for controlled delivery of CDDP.

1. Introduction

Starch, a biodegradable polymer is a promising carrier for drug delivery. It has been used in various fields like biomedical, agriculture and food etc. However, native starch cannot fit into some parental controlled drug delivery systems, as many drugs are released quickly from such unmodified starch-based systems (Michailova et al., 2001); due to considerable swelling and quick enzymatic degradation of native starch in biological systems.

One of the efficacious methods, applied in this study to improve the properties of starch, is the chemical modification of starch which includes esterification. Over the past two decades extensive studies have been conducted on starch ester called as acetylated starch (Wang and Wang, 2002). Chemically transformed starch acetates are less hydrophilic than most of the other modified starches, due to the hydrophobic nature of the acetoxy substituent ($OCOCH_3$). In the drug delivery applications, starch acetate has been extensively used (Korhonen et al., 2004; Nutan et al., 2005, 2007; Pajander et al., 2008; Pohja et al., 2004; Pu et al., 2011; Tuovinen et al., 2004a,b; van Veen et al., 2005; Xu et al., 2009) and tissue engineered scaffold has also been investigated (Guan and Hanna, 2004; Reddy and Yang, 2009).

* Corresponding author. Tel.: +91 9790694972, +91 9789703632.
E-mail address: alaguraj2@rediffmail.com (V. Raj).
Peer review under responsibility of University of Bahrain.

http://dx.doi.org/10.1016/j.jaubas.2015.08.001
1815-3852

In cancer chemotherapy, platinum compounds play an important role. One of the most common anticancer agents is Cisplatin (CDDP), the first generation of platinum based chemotherapy drug. It is used in the treatment of solid tumors including gastrointestinal, head and neck, genitourinary and lung tumors (Kelland, 2007; Boulikas and Vougiouka, 2003).

The clinical application of cisplatin for cancer chemotherapy is still in limited use because of its nonspecific biodistribution and severe side effects. In an attempt to overcome this shortcoming, various studies have been conducted by many groups. They are magnetically mediated controlled delivery systems (Likhitkar and Bajpai, 2012), click chemistry (Huynh et al., 2011), SiO_2/polymer for the controlled release of cisplatin (Czarnobaj and Lukasiak, 2007), platinum-tethered gold nanoparticle (Brown et al., 2010). Chemotherapy with cisplatin is connected with some serious side effects, such as: vomiting, nephrotoxicity, ototoxicity, neuropathy, anemia and nausea (Uchino et al., 2005). Owing to these side effects other methods of administering cisplatin are required. In the present study, CSA/PEG/G has been chosen as the raw material to prepare the drug carrier.

The key objective of the current study is to encapsulate the anticancer drug cisplatin (CDDP) into Cassava starch acetate/polyethylene glycol/gelatin (CSA/PEG/G) nanocomposites through the interaction between cisplatin (CDDP) and CSA/PEG/G nanocomposites. Gelatin is a naturally occurring biodegradable macromolecule with well-documented biocompatible properties over other synthetic polymers that make it an appropriate material to be used as a nanoparticulate carrier (Lai et al., 2006). To develop the microspheres, nanoparticles and polymers, Polyethylene glycol (PEG), a suitable graft-forming polymer, has been extensively employed in pharmaceutical and biomedical fields (Jeong et al., 2008). The viability of CDDP-loaded polymeric nanocomposites as a drug delivery system was verified by evaluating its in vitro studies and instrumental characteristics.

2. Materials and methods

2.1. Materials

Native Cassava starch powder was obtained from Sago Serve Industries (Salem, India). Acetic acid ($\geqslant$99%) and acetic anhydride ($\geqslant$98%) were of analytical grade procured from Sigma–Aldrich (St. Louis, USA). PEG 10000, gelatin Type-B, phosphate-buffered saline (PBS) were prepared in deionized water using NaCl (0.14 M), KCl (2.68×10^{-3} M), Na_2HPO_4 (0.01 M), KH_2PO_4 (1.76×10^{-3} M). Sodium hydroxide (NaOH) and absolute ethanol were purchased from Merck (Mumbai, India Ltd). Cisplatin was obtained from Dabur Pharma Ltd. (New Delhi, India). All chemicals were used without additional purification.

2.2. Preparation of cassava starch acetate

Native cassava starch was permitted to react with acetic anhydride (1:4 ratio) with pyridine as a catalyst as previously described (Singh and Nath, 2012) with few modifications. Before acetylation, cassava starch was dried in an oven for 20 h at 45–60 °C. Dried starch (25 g) was mixed with acetic anhydride (100 g) through the medium of pyridine (200 g). The reaction was carried out at 120 °C for a period of 3 h. The final product was precipitated with ethanol, filtered and dried in vacuum oven. Lastly, the modified starch was milled and sifted in a sieve (#50 mesh) to obtain a homogeneous particle size and stored in desiccators until further study.

2.3. Preparation of CSA–CDDP nanorods

The CSA nanorods were prepared by a simple nanoprecipitation technique as reported by Chin et al., 2011 with slight modification. CSA (10 mg) was dissolved in 8:10 wt% of NaOH/urea (NU) solution mixtures; this solution mixture was used as a solvent system for the dissolution of acetylated cassava starch. Cisplatin was dissolved in CSA solution and prepared at various concentrations i.e., 10%, 20%, 30%, 40% and 50%, using 4, 8, 12, 16 and 20 mg of drug, respectively. An aliquot of CSA solution (10 mg/mL) containing the various concentrations of the drugs was added drop-wise into a 10 ml of absolute ethanol solution, which was constantly stirred using a magnetic stirrer at a constant stirring rate (1500 rpm). The CSA nanorods were made immediately. This dispersion of nanorods was vacuum evaporated to remove the organic solvent fully. Finally the resultant mixture was centrifuged at 13,000 rpm and the supernatant was removed to obtain the CSA-cisplatin nanorods and freeze-dried at −40 °C for 20 h.

2.4. Preparation of the CSA–CDDP–PEG and CSA–CDDP–PEG–G nanocomposites

The various percentage of encapsulated CSA–CDDP in the PEG and G solution were prepared by a method described in our previous report (Rajan et al., 2013) as follows. First, 10% of PEG solution was prepared in water. Then, the solution was gradually added to a correct portion of the CSA–CDDP nanorods under constant magnetic stirring at room temperature for 1 h. The resulting encapsulated nanocomposites (CSA–CDDP–PEG) were collected by centrifugation at 1500 rpm and freeze-dried at −30 °C for 20 h. Later gelatin (20 mg) was dissolved in water in a similar manner and gradually added to CSA–CDDP–PEG nanocomposites under constant magnetic stirring at room temperature for 1 h. Finally the resulting encapsulated nanocomposites (CSA–CDDP–PEG–G) were collected by centrifugation at 1500 rpm and freeze-dried at −30 °C for 20 h.

2.5. Particle size analysis

Drug loaded polymeric nanocomposites were characterized for the particle size, size distribution and zeta potential using Zetasizer (Malvern Instruments, UK).

2.6. Scanning electron microscopy (SEM) and Fourier transform infrared spectroscopy (FT-IR) analysis

Morphological characteristics of the freshly prepared (CSA–CDDP, CSA–CDDP–PEG, and CSA–CDDP–PEG–G) nanocomposites were viewed using scanning electron microscopy (SEM-Hitachi-S-2700), FT-IR spectrum was taken to study the interaction between polymers and drug using Perkin Elmer spectrum RXI. KBr pellets were concisely prepared by

mixing 1 mg of the sample with 200 mg of KBr. Fourier Transform Infrared spectroscopy (400–4000 cm^{-1}) was performed with a resolution of 2 cm^{-1}.

2.7. TEM analysis

The shape and morphology of the Cisplatin loaded CSA, CSA–PEG and CSA–PEG–G nanocomposites were investigated by transmission electron microscopy (TEM, Hitachi H-600-II) operated at 200 kV.

2.8. Determination of encapsulation efficiency (EE) and loading capacity (LC)

The suspensions of the drug-loaded polymeric nanocomposites were centrifuged at 17,000 rpm for 40 min and the EE and LC of drug loaded polymeric nanocomposites were determined by quantifying the absorption of the clear supernatant using a UV-spectrophotometer (Elico SL 159, India). The corresponding calibration curves were made by testing the supernatant of blank polymeric nanocomposites. Tests were performed in triplicate for each sample. The absorbance value of CDDP was measured using a UV–vis spectrophotometer at the wavelength of 290 nm. The percentage of encapsulation efficiency and loading capacity of CDDP in the CSA, CSA–PEG and CSA–PEG–G nanocomposites are determined by the following equations (Eqs. (1) and (2)), respectively, as reported earlier (Papadimitriou et al., 2008), which are as follows:

$$EE = (W_t - W_f)/W_t \times 100\% \quad (1)$$

$$LC = (W_t - W_f)/W_n \times 100\% \quad (2)$$

where W_t is the total amount of CDDP; W_f is the amount of free CDDP in the supernatant after centrifugation; and W_n is the weight of polymeric nanocomposites after freeze-drying. All measurements were made in triplicate and the average value was reported.

2.9. Evaluation of in vitro drug release

The in vitro drug release tests were carried out on all formulations (2%, 4%, 6%, 8%, and 10% drug loaded samples). Nearly 0.1 mg of each sample was suspended in a definite volume (10 ml) of phosphate buffer saline (PBS) at various pH at 37 °C. The resulting suspension was placed in an incubated shaker at 120 rpm for a definite time period (1 h) and five-milliliter aliquots were taken out of the dissolution medium at appropriate time intervals (30 min), replaced by same volume of fresh PBS buffer, to keep the volume of the release medium constant. The amount of drug released was observed by UV spectrophotometer (Systronics, India) at 290 nm.

3. Results and discussion

3.1. Characterization of polymeric nanocomposites

3.1.1. Preparation and characterization of CDDP loaded polymeric nanocomposites

Table 1 represents the particle size and zeta potentials of the CDDP loaded polymeric nanocomposites. The size of the nanocomposites increases slightly with an increase in the % of CDDP encapsulation. The size of the nanocomposites, which is increased once again, is due to the coordination of PEG and G with CSA–CDDP. The 10% of CDDP loaded CSA, CSA–PEG, CSA–PEG–G nanocomposites displayed a mean particle size value of 143,239 and 311 nm respectively as shown in (Table 1).

Zeta potential tells about the charge on the surface of the polymeric nanocomposites and plays an important role in the stability of the particles in suspension through the electrostatic repulsion between the particles (Wilson et al., 2011). The repulsion among the polymeric nanocomposites with the same type of surface charge provides extra stability (Zhao et al., 2010). The 10% of CDDP loaded CSA, CSA–PEG, CSA–PEG–G nanocomposites exhibited a mean zeta potential value of −24.6 mV, −15.3 mV and −10.0 mV, respectively (Table 1) that lies in the stable range indicating that the prepared nanocomposite systems were stable. The negative values obtained for the zeta potential indicate that the polymeric nanocomposites surface is negatively charged. This negative charge may be due to the availability of the free acetyl groups on the polymer. Negative zeta potential values are detected in all cases, suggesting that CSA chains are primarily located on the surface of the particles. All the zeta potential experiments were done in the aqueous medium after centrifuging the nanocomposites at 15,000 rpm for 30 min and dispersed in millipore water.

3.1.2. Fourier transmission infrared spectroscopy (FT-IR) analysis

The FT-IR spectra of native and acetylated cassava starch are given in Fig. 1. In the spectrum of native starch, there are some discernible absorbencies at 1157, 1016 cm^{-1}, which are attributed to C–O bond stretching (Goheen and Wool, 1991). Other characteristic absorption bands at 928, 859, 765, and 576 cm^{-1} are due to the whole anhydroglucose ring stretching vibrations (Cherif Ibrahima Khalil et al., 2011). The very broad band between 3000–3600 cm^{-1} and 2931 cm^{-1} corresponds to OH and CH stretching respectively (Kacurakova and Wilson, 2001) while the peaks at 1648 cm^{-1} and 1420 cm^{-1} correspond to δ (OH) and δ (CH) bendings (Mano et al., 2003). Compared to native starch, starch acetates had a strong absorption band at 1730 cm^{-1} that is attributed to the stretching vibration of the ester carbonyl C═O and indicated the acetylation of starch.

FT-IR spectra of various CSA–CDDP, CS–CDDP–PEG, and CSA–CDDP–PEG–G nanopolymer composites are shown in Fig. 2a. The CSA spectra exhibited band at 1730 cm^{-1} relative to the stretching of the ester carbonyl (C═O) group of acetylated cassava starch. The addition of PEG and gelatin led to bands at 1666 cm^{-1} relative to the stretching of the ester carbonyl group (Lin et al., 2007). Thus the shift in the peak toward a lower field than the actual field indicates the physical mixture of CSA, PEG, and gelatin. The amino peak of gelatin in the polymer composite was shifted from 1542 to 1547 cm^{-1}. The amide I absorption was primarily due to the stretching vibration of the C–O bond and the amide II band was due to the coupling of the bending of the N–H bond and the stretching of the C–N bond. This result proves that there is an interaction between the CSA and the amino groups of gelatin.

Furthermore, strong characteristic peaks of CDDP are not sensed at the same position in the drug-loaded nanocompos-

Table 1 The particle size and zeta potential values of CSA–CDDP, CSA–CDDP–PEG and CSA–CDDP–PEG–G.

% of CDDP concentration	Particle size (nm) mean ± SD[a]			ZP (mV) mean SD[a]		
	CSA–CDDP	CSA–CDDP–PEG	CSA–CDDP–PEG–G	CSA–CDDP	CSA–CDDP–PEG	CSA–CDDP–PEG–G
10	143.2 ± 12.5	239.0 ± 11.8	311.7 ± 05.0	−24.6 ± 1.1	−15.3 ± 1.4	−10.0 ± 2.0
20	154.4 ± 12.7	245.5 ± 05.8	325.4 ± 10.1	−22.3 ± 1.5	−13.5 ± 1.7	−08.1 ± 1.1
30	168.0 ± 08.6	261.3 ± 15.3	333.6 ± 12.4	−20.1 ± 2.2	−13.0 ± 1.5	−07.3 ± 3.2
40	185.5 ± 11.3	270.1 ± 10.1	345.3 ± 10.3	−18.8 ± 1.5	−11.2 ± 2.3	−06.1 ± 1.4
50	193.2 ± 12.5	274.8 ± 13.6	350.1 ± 07.2	−19.5 ± 1.8	−10.4 ± 1.4	−05.5 ± 1.5

CDDP: Cisplatin; CSA: Cassava starch acetate; PEG: polyethylene glycol; G: gelatin; SD: standard deviation for three determinations.
[a] $n = 3$. The experiments were repeated twice.

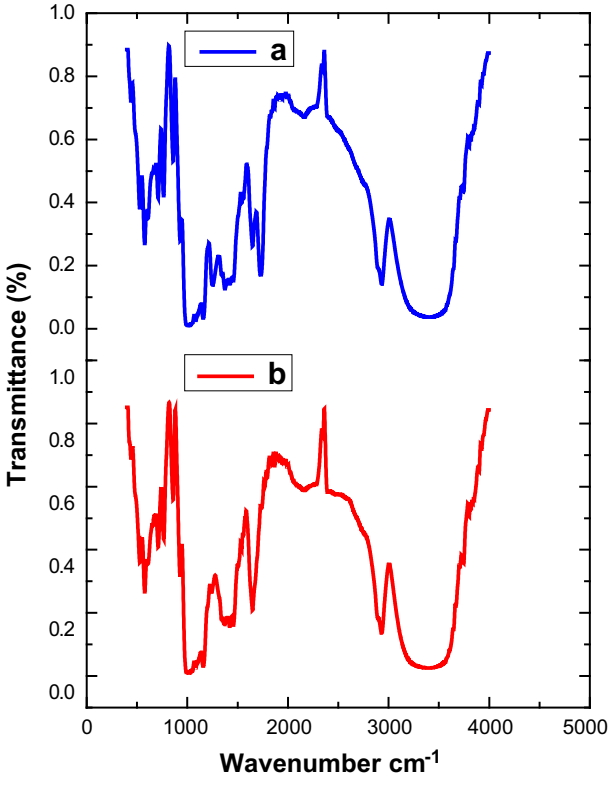

Figure 1 FTIR spectra of (a) acetylation of cassava starch, (b) native cassava starch.

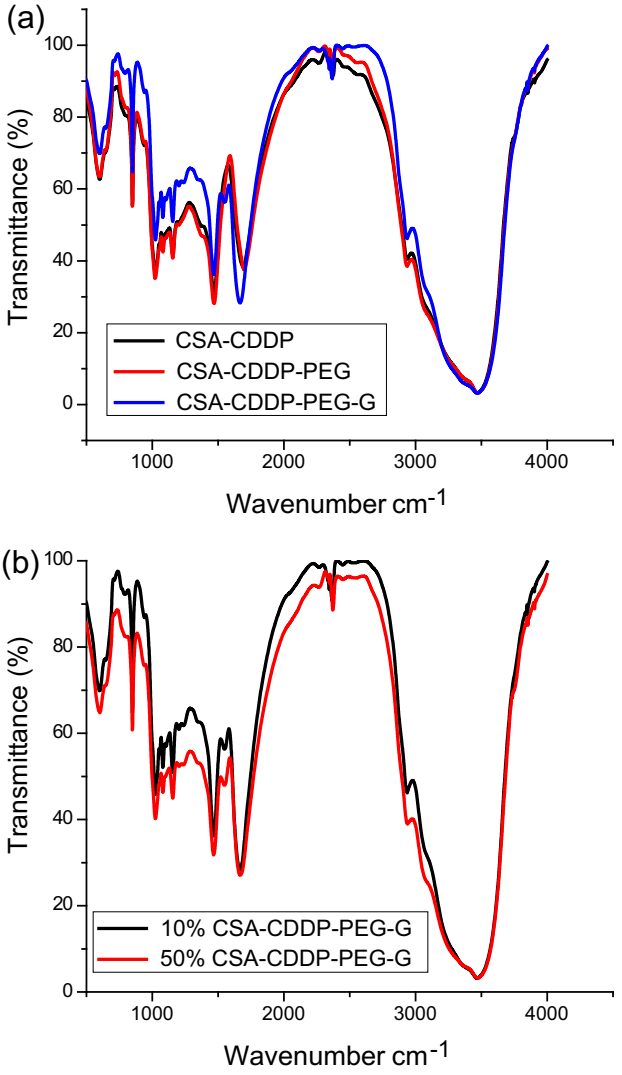

Figure 2 FTIR spectra of (a) and (b) cisplatin loaded nanocomposites.

ites, identifying an interaction between the drug and the polymer composites. Also, the peaks were shifted toward a lower field than the actual field, and this shift was due to the hydrogen bond in the encapsulated polymer composites. Fig. 2b indicates the FT-IR spectra of the 10 and 50% of CDDP coated CSA–CDDP–PEG–G polymeric nanoparticles. The spectra of the coated polymeric nanoparticles displayed the same peaks that vary only in intensity.

3.1.3. Scanning electron microscopy (SEM) of drug loaded polymeric nanocomposites

The SEM images of CSA–CDDP, CSA–CDDP–PEG and C SA–CDDP–PEG–G nanocomposites are shown in Fig. 3.

In addition, the combination of CDDP with nanocomposites produced a smooth surface and compact structure Fig. 3b and c. Particle accumulation and a smooth surface can be seen in the SEM of the secondary mixed-film due to the physical mixture of PEG and G to the CSA. The mixture of CSA with CDDP exhibited certain immiscibility. A clear uniform surface of the G cross-linked polymer composite is shown in Fig. 3c. The coating lying of CDDP with CSA exposed a rough surface. The coating lying of PEG with gela-

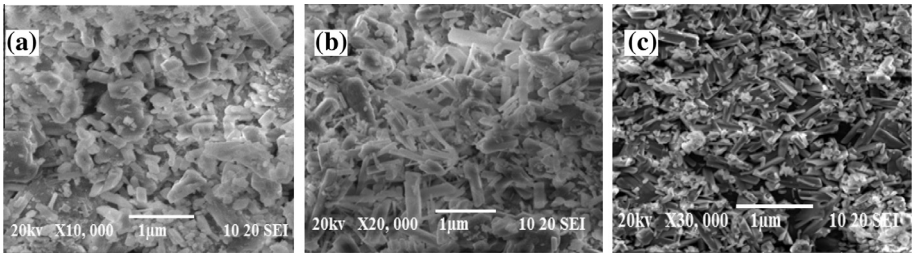

Figure 3 SEM images of cisplatin loaded (a) CSA, (b) CSA–PEG, (c) CSA–PEG–G nanocomposites.

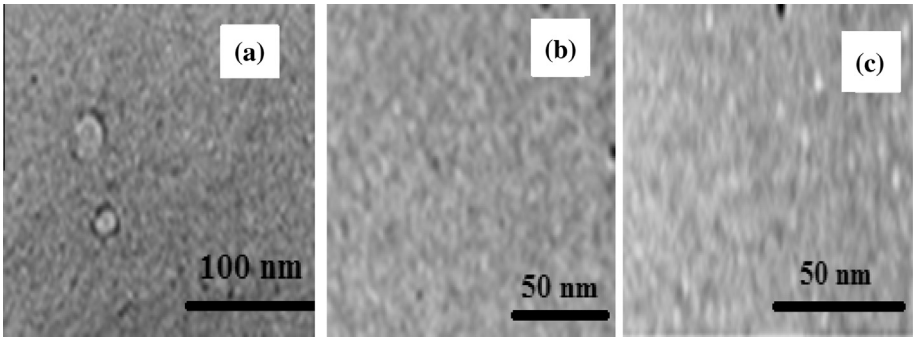

Figure 4 TEM images of cisplatin loaded (a) CSA, (b) CSA–PEG, (c) CSA–PEG–G nanocomposites.

Table 2 Encapsulation efficiency (EE) and loading capacity (LC) of CSA–CDDP, CSA–CDDP–PEG and CSA–CDDP–PEG–G nanocomposites.

% of CDDP concentration	CSA–CDDP nanocomposites		CSA–CDDP–PEG nanocomposites		CSA–CDDP–PEG–G nanocomposites	
	% of EE	% of LC	% of EE	% of LC	% of EE	% of LC
10	23.9	05.3	45.3	10.1	66.9	14.9
20	62.3	22.7	75.5	27.4	84.0	30.5
30	75.4	34.8	85.5	39.4	90.4	41.7
40	82.0	43.8	89.4	47.7	93.6	49.2
50	85.9	50.6	91.6	53.9	94.1	57.0

tin revealed a smoother surface and rod shaped structure, displaying an enhanced encapsulation efficiency and a more consistent structure.

3.1.4. Transmission electron microscopy (TEM) analysis

The surface morphology of the Cisplatin loaded CSA, CS–PEG, and CSA–PEG–G nanocomposites was observed by TEM as shown in Fig. 4. Fig. 4a–c illustrates that the CSA–CDDP, CSA–CDDP–PEG, CSA–CDDP–PEG–G nanocomposites have spherical morphology and are homogeneously distributed with an average diameter of 50–100 nm.

3.2. Encapsulation efficiency (EE) and loading capacity (LC)

The initial concentration of CDDP played a significant role in deciding the drug encapsulation efficiency (EE) and drug loading capacity (LC) of the CSA, CSA–PEG and CSA–PEG–G nanocomposites as shown in Table 2. When the concentration of CDDP is increased, the EE & LC of CSA, CSA–PEG and CSA–PEG–G nanocomposites is also increased. The EE & LC of CSA–PEG–G nanocomposites is somewhat more than that of the CSA and CSA–PEG nanocomposites when at the initial concentration of CDDP is same, which might be accredited to the fact that CSA–PEG–G nanocomposites have more attraction than CSA and CSA–PEG nanocomposites with CDDP. The drug encapsulation efficiency (EE) and drug loading capacity (LC) of high percentage of (50%) CDDP loaded CSA, CSA–PEG & CSA–PEG–G nanocomposites were found to be 85.9%, 91.6% & 94.1% and 50.6%, 53.9%, &57.0%, respectively (Table 2).

3.3. In vitro drug release studies

In vitro drug release studies were done via direct dispersion method as explained in the literature (Bisht et al., 2007; Anitha et al., 2011) at pH 3.4 & 7.4 and release pattern is shown in Fig. 5. The percentage release of CDDP from CSA was slightly greater when compared to that of CSA–PEG and CSA–PEG–G combined nanocomposites. For the CSA–CDDP, CSA–CDDP–PEG and CSA–CDDP–PEG–G coated nanocomposites, the percentage of CDDP released from the nanocomposites was initially much larger and then very slow after some hours, similar to that reported by other authors (Li et al., 2008; Chen et al., 2009, 2011; Yang et al., 2008;

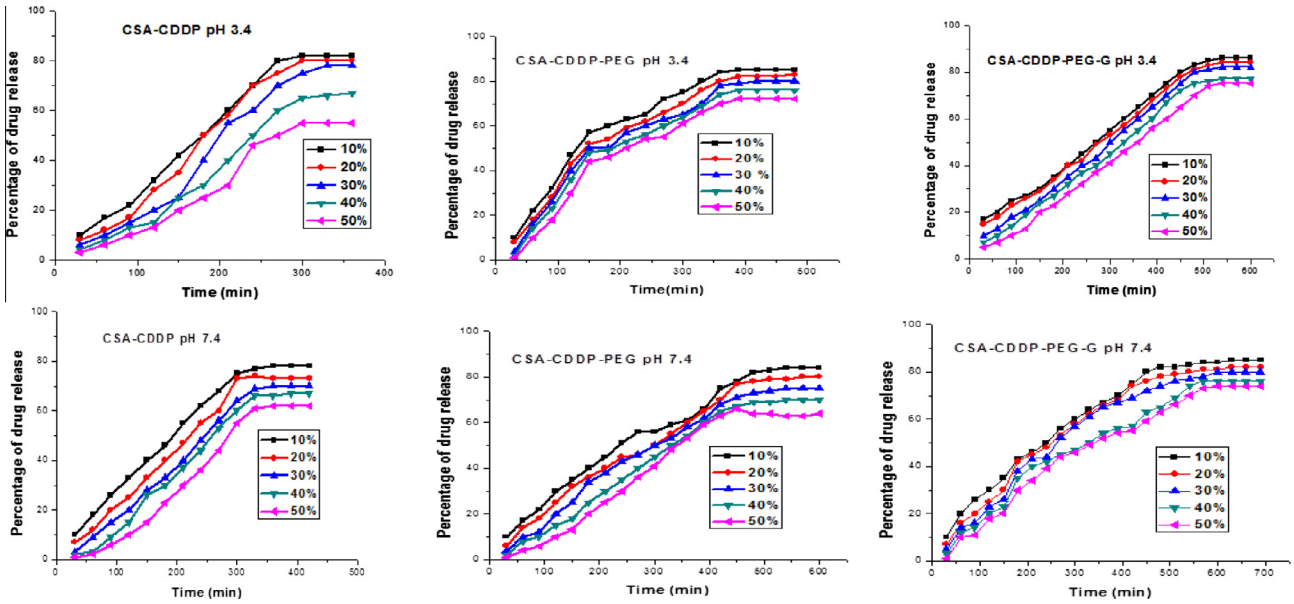

Figure 5 In vitro analysis of cisplatin encapsulated nanocomposites.

Zhang et al., 2009). Fig. 5 shows the release profile at both the pH for the same drug loading, as the pH value of the releasing buffer increased, the releasing rate of CDDP increased. From Fig. 5, we also found that the release rate of the CDDP which was loaded in the CSA, CSA–PEG and CSA–PEG–G loaded nanocomposites was much lower than the free CDDP. The results indicated that the release of CDDP from CSA, CSA–PEG and CSA–PEG–G nanocomposites is pH dependant, the CDDP released faster in acidic environment than at basic environment as a consequence of binding between drug and the carboxyl group in cassava starch acetate nanocomposites which could be recovered by the attacking of H^+ or Cl^-. At body environment, the Cl^- concentration is very high (95–105 mM) and relatively stable in body circulation, more acidic environment means more H^+ which can speed up the release of CDDP from the coated polymeric nanocomposites.

4. Conclusions

In this study, a novel formulation of CDDP loaded CSA, CSA–PEG, CSA–PEG–G nanocomposites was successfully developed and characterized. Size and shape of the prepared nanocomposites were examined using SEM and TEM. Also, the various suspended groups present in the composites have been determined through the FT-IR studies. The nanocomposites showed pH and time dependent drug release as confirmed by the in vitro drug dissolution profiles. Drug penetration and in vitro tests suggest that further study is required to develop an in vivo drug delivery system. These results suggest that the CDDP coated CSA, CSA–PEG and CSA–PEG–G nanocomposites might be used as great potential carriers for controlled drug delivery system.

Acknowledgements

One of the authors (G. Prabha) would like to acknowledge the National Centre for Nanoscience and Nanotechnology, University of Madras, Chennai, India for providing the necessary instrumental facilities and the dedicated support of C. Vijayabhaskar.

References

Anitha, A., Maya, S., Deepa, N., Chennazhi, K.P., Nair, S.V., Tamura, H., 2011. Efficient water-soluble biodegradable polymeric nanocarrier for the delivery of curcumin to cancer cells. Carbohydr. Polym. 83, 452–461.

Bisht, S., Feldmann, G., Soni, S., Ravi, R., Karikar, C., Maitra, M., 2007. Polymeric nanoparticle-encapsulated curcumin (“nanocurcumin”): a novel strategy for human cancer therapy. J. Nanobiotechnol. 5, 3. http://dx.doi.org/10.1186/1477-3155r-r5-3.

Boulikas, T., Vougiouka, M., 2003. Cisplatin and platinum drugs at the molecular level. Oncol. Rep. 10, 1663–1683.

Brown, S.D., Nativo, P., Smith, J.A., Stirling, D., Edwards, P.R., Venugopal, B., Flint, D.J., Plumb, J.A., Graham, D., Wheate, N.J., 2010. Gold nanoparticles for the improved anticancer drug delivery of the active component of oxaliplatin. J. Am. Chem. Soc. 132 (13), 4678.

Chen, H.L., Yang, W.Z., Chen, H., Liu, L.R., Gao, F.P., Yang, X.D., 2009. Surface modification of mitoxantrone-loaded PLGA nanospheres with chitosan. Colloids Surf. B 73, 212–218.

Chen, M., Liu, Y., Yang, W., Li, X., Liu, L., Zhou, Z., 2011. Preparation and characterization of self-assembled nanoparticles of 6-O-cholesterol-modified chitosan for drug delivery. Carbohydr. Polym. 84, 1244–1251.

Cherif Ibrahima Khalil, D., Hai Long, L., Bi Jun, X., John, S., 2011. Effects of acetic acid/acetic anhydride ratios on the properties of corn starch acetates. Food Chem. 26, 1662–1669.

Chin, S.F., Pang, S.C., Tay, S.H., 2011. Size controlled synthesis of starch nanoparticles by a simple nanoprecipitation method. Carbohydr. Polym. 86, 1817–1819.

Czarnobaj, K., Lukasiak, J., 2007. In vitro release of cisplatin from sol–gel processed organically modified silica xerogels. J. Mater. Sci. – Mater. Med. 18 (10), 2041.

Goheen, S.M., Wool, R.P., 1991. Degradation of polyethylene starch blends in soil. J. Appl. Polym. Sci. 42, 2691–2701.

Guan, J., Hanna, M.A., 2004. Extruding foams from corn starch acetate and native corn starch. Biomacromolecules 5 (6), 2329–2339.

Huynh, V.T., Chen, G., Souza, P., Stenzel, M.H., 2011. Thiol-yne and Thiol-ene "Click" chemistry as a tool for a variety of platinum drug delivery carriers, from statistical copolymers to crosslinked micelles. Biomacromolecules 12 (5), 1738–1751.

Jeong, Y., Kim, D.G., Jang, M.K., Nah, J.W., 2008. Preparation and spectroscopic characterization of methoxy poly (ethylene glycol)-grafted water-soluble chitosan. Carbohydr. Res. 343, 282–289.

Kacurakova, M., Wilson, R.H., 2001. Developments in mid-infrared FTIR spectroscopy of selected carbohydrates. Carbohydr. Polym. 44, 291–303.

Kelland, L., 2007. The resurgence of platinum-based cancer chemotherapy. Nat. Rev. Cancer 77, 573–584.

Korhonen, O., Kanerva, H., Vidgren, M., Urtti, A., Ketolainen, J., 2004. Evaluation of novel starch acetate-diltiazem controlled release tablets in healthy human volunteers. J. Controlled Release 95 (3), 515–520.

Lai, J.Y., Lu, P.L., Chen, K.H., Tabata, Y., Hsiue, G.H., 2006. Effect of charge and molecular weight on the functionality of gelatin carriers for corneal endothelial cell therapy. Biomacromolecules 7, 1836–1844.

Li, X.L., Li, R.T., Qian, X.P., Ding, Y.T., Tu, Y.X., Guo, R., Hu, Y., Jiang, X.Q., Guo, W.H., Liu, B.R., 2008. Superior antitumor efficiency of cisplatin-loaded nanoparticles by intratumoral delivery with decreased tumor metabolism rate. Eur. J. Pharm. Biopharm. 70, 726–734.

Likhitkar, S., Bajpai, A.K., 2012. Magnetically controlled release of cisplatin from superparamagnetic starch nanoparticles. Carbohydr. Polym. 87, 300–308.

Lin, Y., Chen, Q., Luo, H., 2007. Preparation and characterization of N-(2-rboxybenzyl) chitosan as a potential pH-sensitive hydrogel for drug delivery. Carbohydr. Res. 342, 87–94.

Mano, J.F., Koniarova, D., Reis, R.L., 2003. Thermal properties of thermoplastic starch/synthetic polymer blends with potential biomedical applicability. J. Mater. Sci. – Mater. Med. 14, 127–135.

Michailova, V., Titeva, St., Kotsilkova, R., Krusteva, E., Minkov, E., 2001. Influence of hydrogel structure on the processes of water penetration and drug release from mixed hydroxypropylmethyl cellulose/thermally pregelatinized waxy maize starch hydrophilic matrices. Int. J. Pharm. 222, 7–17.

Nutan, M.T., Soliman, M.S., Taha, E.I., Khan, M.A., 2005. Optimization and characterization of controlled release multi-particulate beads coated with starch acetate. Int. J. Pharm. 294 (1–2), 89–101.

Nutan, M.T., Vaithiyalingam, S.R., Khan, M.A., 2007. Controlled release multiparticulate beads coated with starch acetate: material characterization, and identification of critical formulation and process variables. Pharm. Dev. Technol. 12 (3), 307–320.

Pajander, J., Soikkeli, A.M., Korhonen, O., Forbes, R.T., Ketolainen, J., 2008. Drug release phenomena within a hydrophobic starch acetate matrix: FT-IR mapping of tablets after in vitro dissolution testing. J. Pharm. Sci. 97 (8), 3367–3378.

Papadimitriou, S., Bikiaris, D., Avgoustakis, K., Karavas, E., Georgarakis, M., 2008. Chitosan nanoparticles loaded with dorzolamide and pramipexole. Carbohydr. Polym. 73, 44–54.

Pohja, S., Suihko, E., Vidgren, M., Paronen, P., Ketolainen, J., 2004. Starch acetate as a tablet matrix for sustained drug release. J. Controlled Release 94 (2–3), 293–302.

Pu, H., Chen, L., Li, X., Xie, F., Yu, L., Li, L., 2011. An oral colon-targeting controlled release system based on resistant starch acetate: synthetization, characterization, and preparation of film-coating pellets. J. Agric. Food Chem. 59 (10), 5738–5745.

Rajan, M., Raj, V., Al-Arfaj, A.A., Murugan, A.M., 2013. Hyaluronidase enzyme core-5-fluorouracil-loaded chitosan-PEG-gelatin polymer nanocomposites as targeted and controlled drug delivery vehicles. Int. J. Pharm. 453, 514–522.

Reddy, N., Yang, Y., 2009. Preparation and properties of starch acetate fibers for potential tissue engineering applications. Biotechnol. Bioeng. 103 (5), 1016–1022.

Singh, A.V., Nath, L.K., 2012. Evaluation of acetylated moth bean starch as a carrier for controlled drug delivery. Int. J. Biol. Macromol. 50 (2), 362–368.

Tuovinen, L., Peltonen, S., Liikola, M., Hotakainen, M., Lahtela-Kakkonen, M., Poso, A., 2004a. Drug release from starch-acetate microparticles and films with and without incorporated alpha-amylase. Biomaterials 25 (18), 4355–4362.

Tuovinen, L., Ruhanen, E., Kinnarinen, T., Ronkko, S., Pelkonen, J., Urtti, A., 2004b. Starch acetate microparticles for drug delivery into retinal pigment epithelium-in vitro Study. J. Controlled Release 98 (3), 407–413.

Uchino, H., Matsumura, Y., Negishi, T., Koizumi, F., Hayashi, T., Honda, T., 2005. Cisplatin–incorporating polymeric micelles (NC-6004) can reduce nephrotoxicity and neurotoxicity of cisplatin in rats. Br. J. Cancer 93, 678–687.

Van Veen, B., Pajander, J., Zuurman, K., Lappalainen, R., Poso, A., Frijlink, H.W., 2005. The effect of powder blend and tablet structure on drug release mechanisms of hydrophobic starch acetate matrix tablets. Eur. J. Pharm. Biopharm. 61 (3), 149–157.

Wang, Y.J., Wang, L., 2002. Characterization of acetylated waxy maize starches prepared under catalysis by different alkali and alkaline earth hydroxides. Starch/Stärke 54, 25–30.

Wilson, B., Samanta, M.K., Muthu, M.S., Vinothapooshan, G., 2011. Design and evaluation of chitosan nanoparticles as novel drug carrier for the delivery of rivastigmine to treat Alzheimer's disease. Ther. Delivery 5, 599–609.

Xu, W., Yang, W., Yang, Y., 2009. Electrospun starch acetate nanofibers: development, properties, and potential application in drug delivery. Biotechnol. Progr. 25 (6), 1788–1795.

Yang, X.D., Zhang, Q.Q., Wang, Y.S., Chen, H., Zhang, H.Z., Gao, F. P., 2008. Self- aggregated nanoparticles from methoxy poly (ethylene glycol)-modified chitosan: synthesis; characterization; aggregation and methotrexate release in vitro. Colloids Surf. B 61, 125–131.

Zhang, H.Z., Gao, F.P., Liu, L.R., Li, X.M., Zhou, Z.M., Yang, X.D., 2009. Pullulan acetate nanoparticles prepared by solvent diffusion method for epirubicin chemotherapy. Colloids Surf. B 71, 19–26.

Zhao, D.M., Zhao, X.H., Zu, Y.G., Li, J.L., Zhang, Y., Jiang, R., Zhang, Z.H., 2010. Preparation, characterization, and in vitro targeted delivery of folate-decorated paclitaxel-loaded bovine serum albumin nanoparticles. Int. J. Nanomed. 5, 669–677.